JOURNAL OF BACTERIOLOGY, Oct. 2007, p. 7503–7506 Vol. 189, No. 20
0021-9193/07/$08.00+0 doi:10.1128/JB.00957-07

Cell Surface Filaments of the Gliding Bacterium *Flavobacterium johnsoniae* Revealed by Cryo-Electron Tomography▽†

Jun Liu,[1] Mark J. McBride,[2]* and Sriram Subramaniam[1]*

Laboratory of Cell Biology, Center for Cancer Research, National Cancer Institute, National Institutes of Health, Bethesda, Maryland 20892,[1] and Department of Biological Sciences, University of Wisconsin—Milwaukee, Milwaukee, Wisconsin 53201[2]

Received 17 June 2007/Accepted 2 August 2007

Flavobacterium johnsoniae **cells glide rapidly over surfaces by an as-yet-unknown mechanism. Using cryo-electron tomography, we show that wild-type cells display tufts of ~5-nm-wide cell surface filaments that appear to be anchored to the inner surface of the outer membrane. These filaments are absent in cells of a nonmotile *gldF* mutant but are restored upon expression of plasmid-encoded GldF, a component of a putative ATP-binding cassette transporter.**

Cells of *Flavobacterium johnsoniae*, and of many other members of the phylum *Bacteroidetes*, move rapidly over surfaces in a process known as gliding motility (12, 13). *F. johnsoniae* cells typically move at speeds of 2 to 5 μm/s over glass surfaces. They also adsorb added latex spheres and propel these around the cell in multiple paths (18). Numerous behavioral, biochemical, electron microscopic, and genetic analyses of *F. johnsoniae* have been conducted to understand gliding, but the structures that comprise the motility machinery and the mechanism of cell movement are not known (1, 6, 7, 12, 13, 16–18). Analysis of the genome sequences of two gliding bacteroidetes, *Cytophaga hutchinsonii* and *F. johnsoniae*, indicated that known motility organelles such as flagella or type IV pili are absent (23).

Genetic analyses have identified 12 cell envelope-associated Gld (gliding) proteins that are required for gliding (2, 4, 5, 8–10, 14, 15). GldA, GldF, and GldG appear to interact to form an ATP-binding cassette (ABC) transporter (8). The cargo of this transporter and its exact role in gliding are not known. GldI is a lipoprotein that is similar to peptidyl-prolyl isomerases involved in protein folding (14). Analysis of the amino acid sequences of the remaining eight Gld proteins (GldB, GldD, GldH, GldJ, GldK, GldL, GldM, and GldN) did not suggest obvious functions (4, 5, 9, 10, 15). Genetic analysis suggests that few if any proteins that are absolutely required for motility remain to be identified (4). The known Gld proteins are thought to be associated with the cytoplasmic membrane, periplasm, and inner face of the outer membrane, suggesting that much of the gliding motility apparatus resides in this region of the cell envelope (2, 4, 5, 8–10, 14, 15). Some of these proteins presumably comprise the gliding motor, which is thought to exert force on cell surface components of the machinery. The cell surface components have not yet been identified by genetic analyses. It is possible they could have been missed because of redundancy in the outer components, such that no single cell surface protein is essential for cell movement.

To explore the structural components of the apparatus for gliding motility, we carried out three-dimensional (3D) imaging of intact, plunge-frozen *F. johnsoniae* cells using cryo-electron tomography, which provides a powerful approach to visualize the architectures of prokaryotic and eukaryotic cells without fixation or staining (21, 25). Cells of wild-type *F. johnsoniae* UW101 (14) were examined and compared to cells of the *gldF* mutant UW102-77 and to cells of UW102-77 complemented with pMK314, which carries the wild-type *gldFG* region (8). UW102-77 has a 2-bp deletion 17 bp downstream of the A residue of the *gldF* start codon (8). In addition to eliminating production of GldF protein, this frameshift mutation is polar on *gldG*, which encodes another component of the *gld* ABC transporter.

Cells for electron tomography analysis were grown in motility medium (MM) consisting of 3.3 g Casitone per liter, 1.7 g yeast extract per liter, and 3.3 mM Tris (pH 7.5). Erythromycin (100 μg/ml) was added to cultures carrying pMK314. Five milliliters of MM in a 125-ml flask was inoculated with cells and incubated overnight at 25°C without shaking until a density of approximately 5×10^8 cells/ml was reached. Cells in MM were examined for motility essentially as previously described (9, 10). Nearly every wild-type cell, and those of the complemented strain, exhibited rapid gliding over glass. In contrast, cells of the *gldF* mutant UW102-77 were completely nonmotile. Four-microliter samples in MM were applied to 3-mm-wide holey carbon grids, plunge-frozen in liquid ethane, and examined using a Polara microscope (FEI Corp., OR) equipped with a field emission gun operating at 300 kV and a 2K-by-2K charge-coupled device camera at the end of a GIF 2000 (Gatan, Inc., Pleasanton, CA) energy filtering system. In some cases, 0.2-μm latex spheres (Seradyn, Indianapolis, IN) were added to the cell suspension. Since these spheres bind to the cell surface and are propelled by the motility machinery, they serve as useful markers to direct attention to regions of the cell surface that are likely to have been actively moving at the time that the cells were plunge-frozen. Low-dose single-

* Corresponding author. Mailing address for S. Subramaniam: Laboratory of Cell Biology, Center for Cancer Research, National Cancer Institute, National Institutes of Health, Bethesda, MD 20892. Phone: (301) 594-2062. Fax: (301) 480-3834. E-mail: ss1@nih.gov. Mailing address for M. J. McBride: Department of Biological Sciences, University of Wisconsin—Milwaukee, Milwaukee, WI 53201. Phone: (414) 229-5844. Fax: (414) 229-3926. E-mail: mcbride@uwm.edu.

† Supplemental material for this article may be found at http://jb.asm.org/.

▽ Published ahead of print on 10 August 2007.

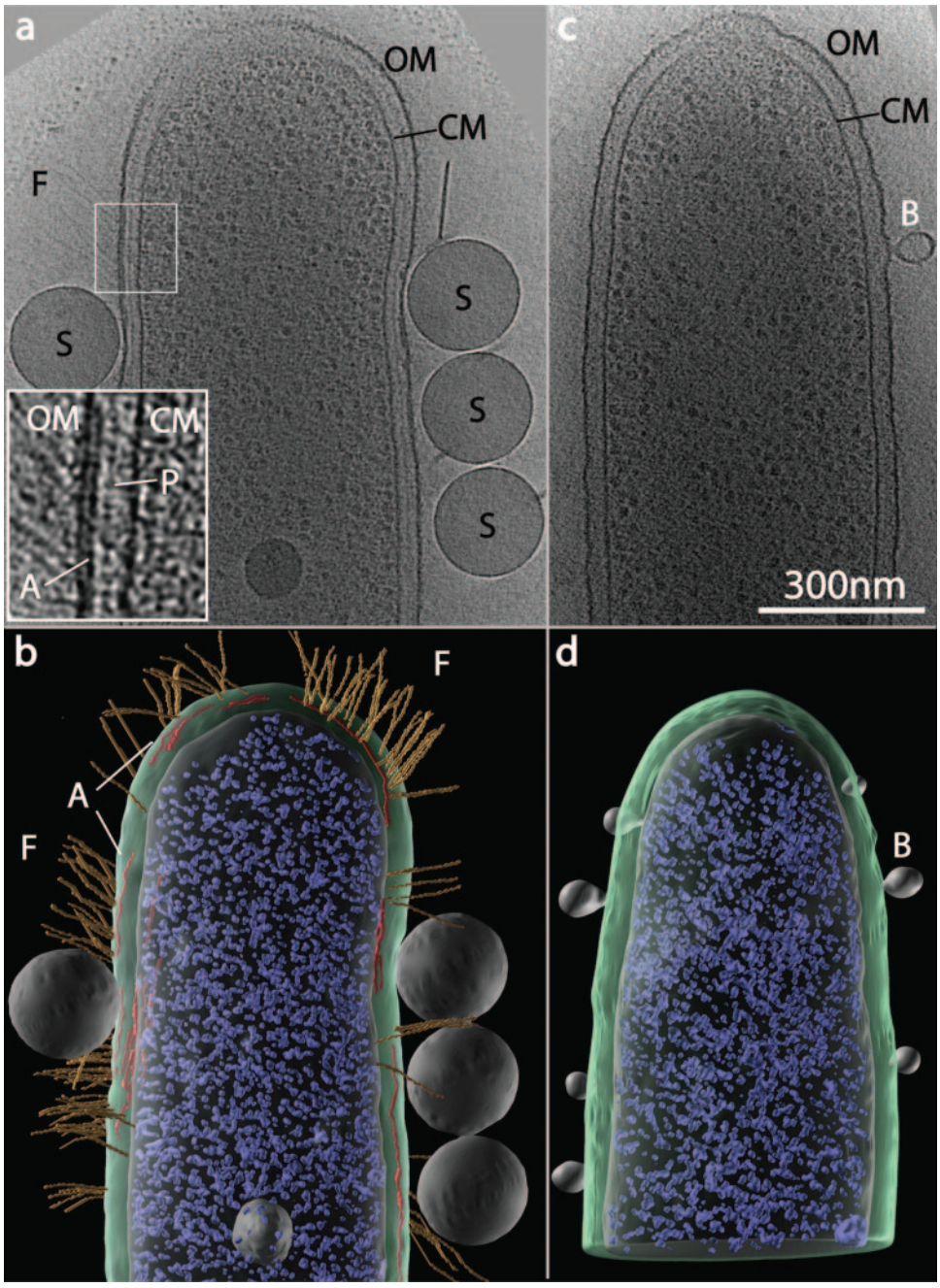

FIG. 1. Cryo-electron tomography of wild-type and mutant *F. johnsoniae* cells. (a) Three-nanometer tomographic slice of a plunge-frozen wild-type cell. Features arising from the cytoplasmic membrane (CM), outer membrane (OM), peptidoglycan (P), cell surface filaments (F), and added latex spheres (S) can be visualized. The inset shows an expanded view of the periplasmic region at a location where filaments are observed. The densities arising from the outer membrane, cytoplasmic membrane, peptidoglycan layer, and patch (A) at the base of the outer membrane can be clearly seen. (b) Segmented representation of a whole wild-type cell in 3D, showing the spatial relationships between the various cellular components. Filaments (yellow), cytoplasmic and outer membranes (gray and light green, respectively), anchoring patches (red), and contributions from putative ribosomes in the cytoplasm (blue) are shown. (c) Three-nanometer tomographic slice from the *gldF* mutant. In this mutant, numerous vesicular blebs (B) are observed on the outer membrane surface. (d) Segmented representation of a *gldF* mutant cell, with color scheme as in panel b.

axis tilt series were collected from frozen-hydrated specimens at liquid nitrogen temperatures in the zero-loss mode at effective magnifications of ×18,000 and with underfocus values of ~6 to 7 μm. The angular range of the tilt series (~90 images) was from −70° to +70° at increments of 1.5°. The cumulative dose of the tilt series was less than 100 $e^{-}/Å^{2}$. Tilt series were initially aligned with gold markers using FEI inspect3D and further refined and reconstructed by weighted back-projection using Protomo (22). The 3D segmentation of cryo tomograms was performed with Amira (Mercury Systems, San Diego, CA).

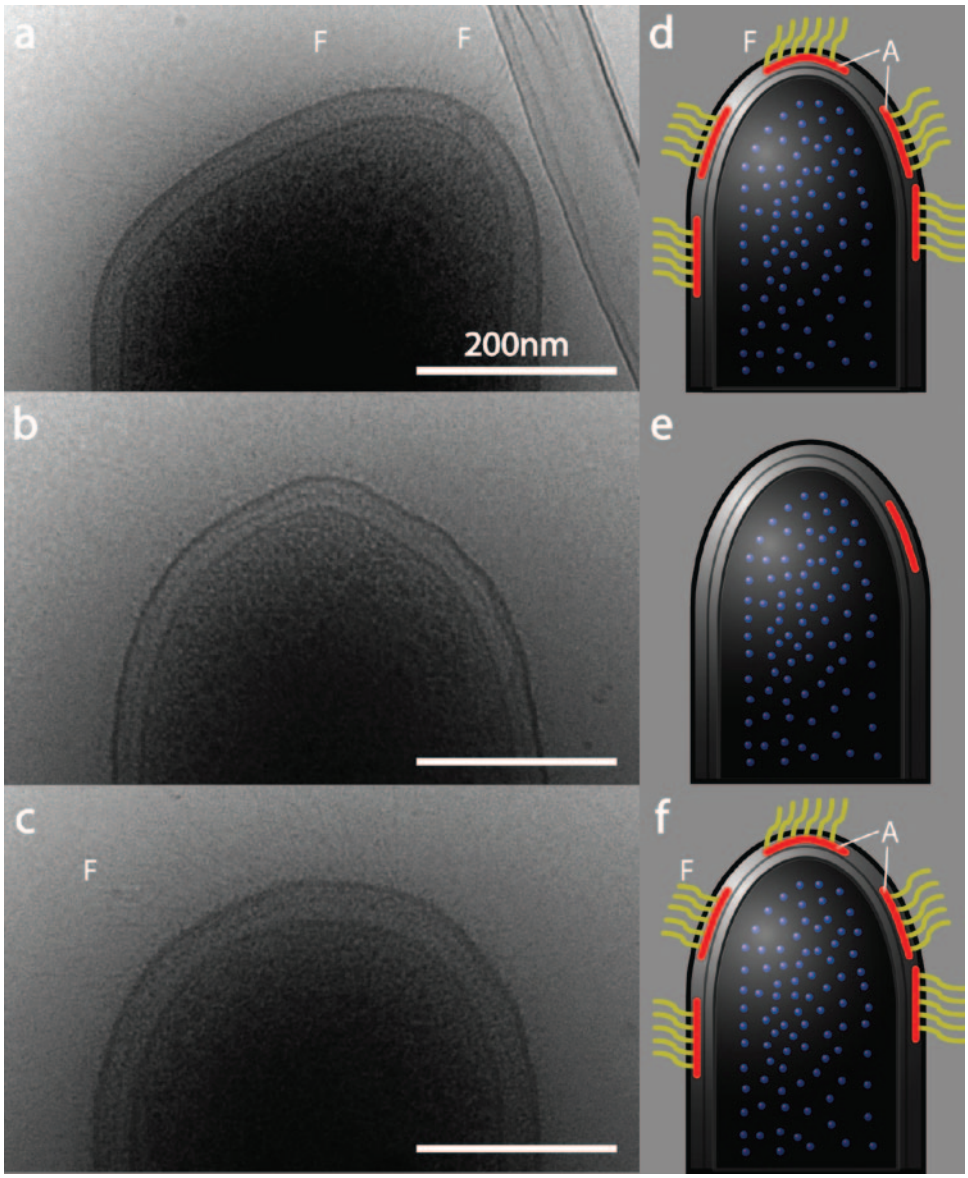

FIG. 2. Restoration of filaments in *gldF* mutant UW102-77 complemented with pMK314. Projection images recorded from plunge-frozen cells of the wild type (a), *gldF* mutant UW102-77 (b), and *gldF* mutant UW102-77 complemented with pMK314 (c). No filaments are observed in the *gldF* mutant, although on rare occasions a patch-like feature was observed near the base of the outer membrane. The expression of wild-type GldF and GldG rescues both function and the observation of cell surface filaments. Filaments (F) in panels a and c are indicated. The schematic models in panels d, e, and f correspond to the data shown in panels a, b, and c, respectively, with the color scheme used in Fig. 1b and d.

As illustrated in Fig. 1, wild-type *F. johnsoniae* cells are ~0.45 μm wide and vary in length from ~5 to ~10 μm. A tilt series was collected from the tip of a representative wild-type cell that had several attached latex spheres and was embedded in thin vitreous ice (Fig. 1). A representative tomographic slice from the interior of the cell shows features characteristic of typical gram-negative bacteria, including densities corresponding to the inner and outer membranes and the peptidoglycan layer. Other features visible include density arising from ribosomes in the cytoplasm, the latex beads attached to the cell surface, and dense granules which may be rich in polyphosphate (M. J. Borgnia, S. Subramaniam, and J. L. S. Milne, unpublished data). A striking feature of 3D reconstructions of wild-type cells (Fig. 1a and b) is the presence of thin filaments extending from the outer membrane (see Movie S1 in the supplemental material). The filaments are typically ~5 nm wide and ~100 nm long and are distributed unevenly on the cell surface. They are somewhat similar in appearance to the spicules of the nonflagellated swimming cyanobacterium *Synechococcus* sp. strain WH8113 (20). The four latex spheres that are associated with the cell shown in Fig. 1a are in close contact with the outer membrane in regions of the cell that also displayed cell surface filaments. In some cases, contact of the spheres with the cell surface appeared to be associated with deformation of the outer membrane (shown more clearly in Movie S1 in the supplemental material).

An interesting feature observed in these cells, but not in *Escherichia coli* cells (24, 25), is the presence of electron-dense patches at the base of the outer membrane (Fig. 1a, inset). This extra layer of density was frequently observed in short, interrupted stretches, in contrast to the continuous densities from the outer membrane, inner membrane, and peptidoglycan layer. Importantly, the presence of the patches was almost always correlated with the presence of the filaments extending outwards from the cell (see Movie S1 in the supplemental material and Fig. 1b). Cells of the *gldF* mutant UW102-77 appeared similar to those of wild-type cells, except that cell surface filaments were absent, outer membrane-associated patches were rarely evident, latex spheres failed to bind, and outer membrane blebs were observed more frequently (Fig. 1c and d and see Movie S2 in the supplemental material). Introduction of pMK314, which carries the wild-type *gldFG* region, into cells of UW102-77 restored gliding motility, cell surface filaments, and the patches at the base of the outer membrane (Fig. 2).

Our key findings are summarized in the cartoons shown in Fig. 2d to f. The correlation between the observation of filaments and the patches of density at the base of the outer membrane is intriguing. All of the Gld proteins characterized to date are associated with the cytoplasmic membrane, periplasm, and inner face of the outer membrane (2, 4, 5, 8–10, 14, 15), so it is unlikely that any of these are components of the cell surface filaments. An interesting possibility is that these filaments, anchored by the patches in the periplasmic space, could be adhesins that contact the substratum. The patches could be components of the motor assembly. They could represent the contribution of mass from the periplasmic domains of the ABC transporter composed of GldA, GldF, and GldG and/or of the abundant outer membrane lipoprotein GldJ (5). Consistent with this idea, disruption of *gldF* results not only in loss of GldF and GldG but also in greatly decreased levels of GldJ lipoprotein, probably as a result of instability of GldJ in the absence of the ABC transporter (5).

Over the last three decades, numerous models have been proposed to explain the mechanism of gliding of *F. johnsoniae* and related bacteria (3, 11, 18, 19). These models generally invoke machinery in the cell envelope that interacts with and propels cell surface adhesins. The studies we report here provide the first direct evidence that the surfaces of *F. johnsoniae* cells contain thin filaments that appear to mediate gliding function and are thus likely to represent the elusive adhesive surface organelles of the *F. johnsoniae* gliding motility machinery.

This research was supported by grants from the intramural research program of the National Cancer Institute to S.S. and by grants from the National Science Foundation (MCB-0130967 and MCB-0641366) and the University of Wisconsin—Milwaukee Research Growth Initiative to M.J.M.

Sequence data for *C. hutchinsonii* and *F. johnsoniae* were obtained from the Joint Genome Institute (http://jgi.doe.gov), Los Alamos National Labs, and the U.S. Department of Energy.

REFERENCES

1. **Abbanat, D. R., E. R. Leadbetter, W. Godchaux III, and A. Escher.** 1986. Sulphonolipids are molecular determinants of gliding motility. Nature **324:** 367–369.
2. **Agarwal, S., D. W. Hunnicutt, and M. J. McBride.** 1997. Cloning and characterization of the *Flavobacterium johnsoniae* (*Cytophaga johnsonae*) gliding motility gene, *gldA*. Proc. Natl. Acad. Sci. USA **94:**12139–12144.
3. **Beatson, P. J., and K. C. Marshall.** 1994. A proposed helical mechanism for gliding motility in three gliding bacteria (order *Cytophagales*). Can. J. Microbiol. **40:**173–183.
4. **Braun, T. F., M. K. Khubbar, D. A. Saffarini, and M. J. McBride.** 2005. *Flavobacterium johnsoniae* gliding motility genes identified by *mariner* mutagenesis. J. Bacteriol. **187:**6943–6952.
5. **Braun, T. F., and M. J. McBride.** 2005. *Flavobacterium johnsoniae* GldJ is a lipoprotein that is required for gliding motility. J. Bacteriol. **187:**2628–2637.
6. **Burchard, R. P.** 1981. Gliding motility of prokaryotes: ultrastructure, physiology, and genetics. Annu. Rev. Microbiol. **35:**497–529.
7. **Godchaux, W., III, M. A. Lynes, and E. R. Leadbetter.** 1991. Defects in gliding motility in mutants of *Cytophaga johnsonae* lacking a high-molecular-weight cell surface polysaccharide. J. Bacteriol. **173:**7607–7614.
8. **Hunnicutt, D. W., M. J. Kempf, and M. J. McBride.** 2002. Mutations in *Flavobacterium johnsoniae gldF* and *gldG* disrupt gliding motility and interfere with membrane localization of GldA. J. Bacteriol. **184:**2370–2378.
9. **Hunnicutt, D. W., and M. J. McBride.** 2001. Cloning and characterization of the *Flavobacterium johnsoniae* gliding motility genes *gldD* and *gldE*. J. Bacteriol. **183:**4167–4175.
10. **Hunnicutt, D. W., and M. J. McBride.** 2000. Cloning and characterization of the *Flavobacterium johnsoniae* gliding motility genes *gldB* and *gldC*. J. Bacteriol. **182:**911–918.
11. **Lapidus, I. R., and H. C. Berg.** 1982. Gliding motility of *Cytophaga* sp. strain U67. J. Bacteriol. **151:**384–398.
12. **McBride, M. J.** 2001. Bacterial gliding motility: multiple mechanisms for cell movement over surfaces. Annu. Rev. Microbiol. **55:**49–75.
13. **McBride, M. J.** 2004. Cytophaga-flavobacterium gliding motility. J. Mol. Microbiol. Biotechnol. **7:**63–71.
14. **McBride, M. J., and T. F. Braun.** 2004. GldI is a lipoprotein that is required for *Flavobacterium johnsoniae* gliding motility and chitin utilization. J. Bacteriol. **186:**2295–2302.
15. **McBride, M. J., T. F. Braun, and J. L. Brust.** 2003. *Flavobacterium johnsoniae* GldH is a lipoprotein that is required for gliding motility and chitin utilization. J. Bacteriol. **185:**6648–6657.
16. **Pate, J. L.** 1985. Gliding motility in Cytophaga. Microbiol. Sci. **2:**289–295.
17. **Pate, J. L.** 1988. Gliding motility in procaryotic cells. Can. J. Microbiol. **34:**459–465.
18. **Pate, J. L., and L.-Y. E. Chang.** 1979. Evidence that gliding motility in prokaryotic cells is driven by rotary assemblies in the cell envelopes. Curr. Microbiol. **2:**59–64.
19. **Ridgway, H. F., and R. A. Lewin.** 1988. Characterization of gliding motility in *Flexibacter polymorphus*. Cell Motil. Cytoskelet. **11:**46–63.
20. **Samuel, A. D., J. D. Petersen, and T. S. Reese.** 2001. Envelope structure of *Synechococcus* sp. WH8113, a nonflagellated swimming cyanobacterium. BMC Microbiol. **1:**4.
21. **Subramaniam, S.** 2005. Bridging the imaging gap: visualizing subcellular architecture with electron tomography. Curr. Opin. Microbiol. **8:**316–322.
22. **Winkler, H., and K. A. Taylor.** 2006. Accurate marker-free alignment with simultaneous geometry determination and reconstruction of tilt series in electron tomography. Ultramicroscopy **106:**240–254.
23. **Xie, G., D. C. Bruce, J. F. Challacombe, O. Chertkov, J. C. Detter, P. Gilna, C. S. Han, S. Lucas, M. Misra, G. L. Myers, P. Richardson, R. Tapia, N. Thayer, L. S. Thompson, T. S. Brettin, B. Henrissat, D. B. Wilson, and M. J. McBride.** 2007. Genome sequence of the cellulolytic gliding bacterium *Cytophaga hutchinsonii*. Appl. Environ. Microbiol. **73:**3536–3546.
24. **Zhang, P., E. Bos, J. Heymann, H. Gnaegi, M. Kessel, P. J. Peters, and S. Subramaniam.** 2004. Direct visualization of receptor arrays in frozen-hydrated sections and plunge-frozen specimens of *E. coli* engineered to overproduce the chemotaxis receptor Tsr. J. Microsc. **216:**76–83.
25. **Zhang, P., C. M. Khursigara, L. M. Hartnell, and S. Subramaniam.** 2007. Direct visualization of *Escherichia coli* chemotaxis receptor arrays using cryo-electron microscopy. Proc. Natl. Acad. Sci. USA **104:**3777–3781.